Obtaining of a PET-CaF_2 hybrid multifilament: non-isothermal crystallization studies

Keywords: poly (ethylene terephthalate), PET, fluorite particles, CaF_2 nanoparticles, microparticles, nanocomposites, composites, multifilament, yarn, dispersing agent

ABSTRACT

Poly(ethylene terephthalate) (PET) has been mixed with fluorite (CaF_2) particles to obtain micro- and nano-composites aiming to obtain an hybrid multifilament. In first term, the use of two montanic waxes and an amide wax as dispersing agents towards the compabilization of the inorganic and organic components of the CaF_2/ PET composite were considered. To do this, non-isothermal crystallization studies by differential scanning calorimetry have been carried out. Moreover, the influence of the CaF_2 particle size and concentration on the thermal properties of the system have been also studied by this technique. Finally, the extrapolation of the results has materialised as a novel PET/CaF_2 hybrid multifilament. Thermal and mechanical properties and molecular weight of the multifilament have been as well evaluated.

INTRODUCTION

Composites in the form of fibre, composed by a polymeric matrix of poly(ethylene terephthalate) (PET), and ceramic micro- and nanoparticles included in the bulk, are interesting for application in technical textiles. The main drawback is the poor affinity between the organic and the inorganic parts (specifically at the interface) that may be translated in dramatic results. Voids at the nanometric scale in the particle surroundings, that result in a high number of rupture points, or a composite with low particle-homogeneity giving a material with internal stresses, are some of those examples[1]. So far, numerous studies towards the enhancement of the mechanical properties of those composite materials have been performed[2–5]. Concretely, the first goal for the preparation of those high-performed fibres would be the study of the inclusion of dispersing agents to evaluate their influence in the dispersion degree of the particles in the polymeric matrix.

Another important aspect is the possibility to obtain high concentrated mixtures containing large amounts of particles, to not only be considered simple additives, but composites or hybrids. Nevertheless, the conditions of the production of multifilaments are usually more restrictive than other processes because a discontinuity in the extruded melt would mean a breakage of the resulting multifilament. Thus, continuity and adequate viscosity are key factors of the extruded material to produce suitable products. The inclusion of particles to polymers decrease the viscosity of the mixture because the particulated materials are more sensitive to degradation as a result of heating, high shear rates and residence times in the process of mixing in the melt state[6]. Consequently, a significant possibility of breaking the continuity of the melt in the extrusion process exists. Continuity of the melt is, at the same time, related with the particle concentration which is inversely proportional to the viscosity of the mixture[7]. For these reasons, particle size and concentration and the chemical nature of the dispersing agent used in the mixture compatibilization (homogeneization), are important factors to be analized.

Composite properties are closely related to the morphology and distribution of the fillers in the polymer matrix, and also to the crystallization behaviour of the polymer matrix after incorporation of fillers[8,9]. Fillers may act as a nucleating or anti-nucleating agents under certain conditions, affecting the crystallization behaviour of the material[10–12]. Therefore, the understanding of those parameters involving crystallization processes may be the key for the optimization of the processing conditions and the properties of the finished products. For example, common spinning rates for polyester POY (Partially Oriented Yarn) production for tailoring textile clothing are enclosed between 2500 and 4500 m/min. Thus, the decrease of the crystallization temperature of the mixture due to a possible anti-nucleating effect of the compounds may affect negatively the spinning process of it, or even hamper the production of multifilament.

Furthermore, inorganic fluorides have a number of uncommon and interesting properties, such as electron-acceptor behaviour, large optical-transmission domain, high resistivity, and anionic conductivity[13,14]. Nanoscale alkaline fluorides and rare-earth doped inorganic nanoscale fluorides have attracted great interest because of their unique optical, electrical and magnetic properties, which result from the size and shape of their particles[13,14]. Known for their dielectric properties, they are widely used in microelectronic devices, as well as in wide-gap insulating over-layers, insulators, cryogenic high-voltage applications, etc. Calcium fluoride or fluorite (CaF_2) is an interesting material due to its high stability, non-hygroscopic behaviour, and as a component of laser materials when doped with rare-earth elements, it is highly transparent over a wide optical region (170–780 nm)[15–17].

In tribology, some nanomaterials have shown interesting results as prospective lubricating materials or for the development of advanced lubrication technology. Concretely, CaF_2 is brittle and do not possesses lubricating properties at low temperature[18]. However, fluorite undergoes a transition to a plastic state and acts as a lubricant when temperature raises, providing self-lubrication in composite materials. Moreover, CaF_2 exhibits effective self-lubrication properties at temperatures of 400ºC as result of its reduced size when used in thin lubricant films or in self-lubricated metal matrixes. Nanomaterials usually experience a dramatically lowering of the melting points compared to the bulk counterparts due to a small-scale effect. Therefore, CaF_2 nanocrystals have been used as effective additives for grease or oil at low temperatures[18].

From the broad range of inorganic fillers, CaF_2 could behave as nucleating or anti-nucleating agent affecting the crystallization behaviour of PET, according to previous studies conducted by the research group[19,20]. Results showed that parameters such as particle size, surface treatment and filler concentration affected the non-isothermal crystallization behaviour of the composite (nucleation).

On the other hand, crystallization behaviour of PET filled with titanium dioxide (TiO_2) after addition of different dispersing agents was another study conducted by some of the authors[11]. An ester of montanic acid with multifunctional alcohols (MAWMA), a partly saponified ester of montanic acid (PSEMA), and an amide wax base on N,N'-bisstearoyl ethylenediamine (AW), were explored as dispersing agents in order to determine their suitability in the polymeric-based system.

In this way, here the effect of dispersing agents on the dispersion of ceramic and nanoceramic particles, when included in PET for composite fibre formation to obtain PET/CaF_2-based micro (MCPs) and nanocomposites (NCPs) including MAWMA, PSEMA and AW as dispersing agents, are studied through non-isothermal crystallization. Differential Scanning Calorimetry (DSC) and

birefringence microscopy are used to determine the non-isothermal crystallization behaviour of the mixtures. Moreover, the effect of the size of CaF_2 when changing from micro- to nano-scale is analysed by calorimetric assays, and the chemical compatibility of the mixture particles/dispersant/polymer was discussed in terms of the change the in glass transition temperature and another thermodynamic parameters. Finally, NCPs are obtained in a Partially Oriented Yarn (POY) multifilaments form. Molecular weight determination, together with the thermal and mechanical studies, are analysed in order to determine the suitability of CaF_2, the dispersing agent types and ratio of the NCP composition for fibre application. The importance of the study relies on the production of an hybrid multifilament with crystallization properties similar to pure polymer which, from the industrial point of view, means that the composite could be thermally processed at conditions similar to PET.

EXPERIMENTAL PART

Materials

Poly(ethylene terephthalate) (PET). PET was provided by ANTEX, S.L. 100% polyester (extra-bright), textile quality was used in the determination of the suitability of the dispersing agent to produce composites. PET provided by La Seda de Barcelona: Artenius Flow 100% PET without additives (bright), PET bottle grade, was used to determine the effect of the particle size and concentration of fluorite and the concentration of dispersing agent.

PET pellets were stored in a vacuum oven at 50°C and 80 mbar to prevent the degradation and the absorption of humidity of polymer.

Fluorite (CaF_2). Micro- and ultrafine sized particles were obtained as described in a previous work[21]. Mean particle size for micro-fluorite obtained by Dynamic Light Scattering (DLS) was 334 nm and for nano-fluorite 110 nm.

Dispersing agents. The dispersing agents were supplied by Clariant: LICOWAX E flakes, an ester of montanic acids with multifunctional alcohols (MAWMA), LICOWAX OP powder, an ester of montanic acids partly saponified with butyleneglycol and the rest with calcium hydroxide (PSEMA), and LICOWAX C powder, an amide wax based on N,N'-Bisstearoylethylene-diamine (AW).

Preparation

PET/CaF_2 composite. Micro and nano-fluorite were used to prepare composites aiming to evaluate the effect of use of the several dispersing agents. Most of the synthesised particles were under the accepted nanometrical boundary, 100 nm, and were loosely agglomerated (**Fig. 1**). Substrates were prepared without and with (2%) of CaF_2 particles in the presence and in the absence of the different dispersing agents (5%). Mixtures were extruded using a Corima extruder Model G-132 A. The conditions for the extrusion were 275ºC and a screw speed of 70 rpm. Resulting composites were stored at 105ºC during 24 hours. Samples were prepared towards the obtaining of a plate shape using a 10T Bench Top press (from Rondol Technology). For this reason, 10 g of the sample was placed in a mold of 10 x 10 x 0.6 mm^3 in the press, temperature was increased up to 290ºC, maintained for 5 minutes at a pressure of 60 kN and cooled down. Finally, all nanocomposites were then rinsed with distilled water and dried.

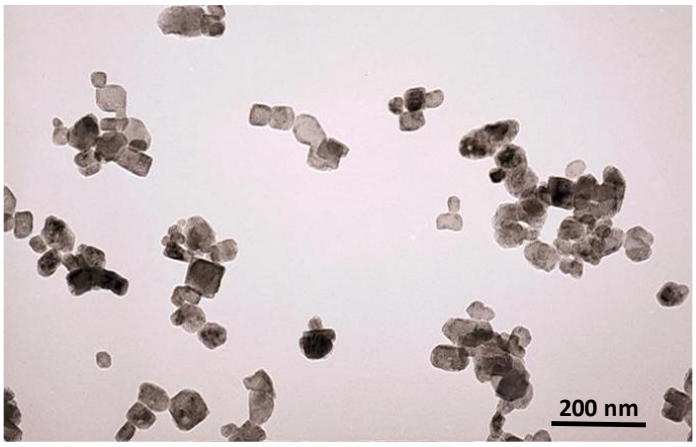

Fig. 1 *TEM micrograph of CaF_2 nanoparticles.*

In a further step, the influence of particle size (nano and micro), and the ratio between CaF_2:dispersing agent concentration in the composite properties, were evaluated (**Table 1**)[21]. The dispersing agent used was the one that showed the most favourable non-isothermal crystallization behaviour.

Table 1. *Composite samples with different CaF_2 sizes and concentrations and dispersing agent concentrations.*

Particle size	Particle concentration (%)	Dispersing agent concentration (%)
Micro-	1	2
	1	4
	2	2
	2	4
	3	2
	3	4
Nano-	1	2
	1	4
	2	2
	2	4
	3	2
	3	4

Multifilament yarn. A PET multifilament yarn containing 2% nanometric CaF_2 and 2% dispersing agent, was prepared and supplied by IQAP Masterbatch Group S.L. The yarn was subsequently stretched at 190ºC at a drawn ratio 1:2 in a laboratory stretching equipment.

Characterization

Differential Scanning Calorimetry (DSC). Thermal analysis tests were performed in a Differential Scanning Calorimeter DSC 7 Perkin Elmer. 7.5 mg of sample were sealed in an aluminium crucible. Temperature program was set according to the experiment developed. Samples were tested by duplicated and results show the mean of them. Non-isothermal crystallization studies were developed under the following conditions: (i) heat up from 40ºC to

290ºC at 300ºC/min, (ii) holding at 290ºC for 5 min, (iii) cool down from 290ºC to 40ºC at 5, 10, 15, and 20ºC/min. Microstructure behaviour of composites was determined according heating up from 40ºC to 300ºC at 20ºC/min. Nitrogen (N_2) purge gas at a flow of 35 ml/min was used for all DSC experiments.

Birefringence Optical Microscopy (BOM). The resulting plates (see PET/CaF_2 composite preparation) were evaluated in an optical microscope Jenalab Pol U – DMC2 and observed under polarized light. The presence of bright "dots" indicates agglomeration of the nanoparticles.

Molecular weight determination. Yarns were previously washed with Sandozina NIA (Clariant) 1 g/L at 35 ± 2°C for 30 minutes and with deionized water at room temperature for 10 minutes three times. Molecular weight determination followed the procedure described in Gacén[22]. Approximately 3 mg of washed yarn were placed in a test tube with 0.2 mL of o-chlorophenol (>99%, Aldrich). The tubes were placed in a polyethylene glycol bath at 80°C for 30 minutes. Once the yarn was dissolved and the tubes cooled, 1.8 mL of chloroform (HPLC grade, stabilized with amylene, aprox. 150 ppm, Scharlau) were incorporated. The mixture was stirred and subsequently, the solution was filtered (PTFE filter, 0.45 μm) and transferred to a vial. Analysis were carry out in high performance liquid chromatograph (Perkin Elmer) provided with Injector model ISS200, 200lc series pump, oven for columns series 200, refractive index detector Series 200a. The separation was performed at 40ºC with chloroform (HPLC grade, Scharlau), at a flow rate of 1 mL/min on PLgel 5 μm Mixed-D column 300 x 7.5 mm (Agilent), using a Oligopore Column 6 μm 300 x 7.5 mm (Agilent). The system was calibrated with polystyrene standards with weight average molecular weight in the range 2350 - 200000 g/mol (Waters). The software TotalChrom Navigator – TurboSEC v. 6.3.1.0504 was used to calculate molecular weight in number, molecular weight in number in weight and polydispersity.

Lineal density determination. Before the test, yarns were conditioned according to UNE-EN 13392: 2001. For the determination of the count, 100 m of each yarn were collected in the Aspe JBA. Subsequently, samples were weighted on an analytical balance (± 0.1 mg) and the relationship between mass and length was calculated. This procedure was performed for each sample by triplicate.

Tenacity determination. Tensile tests were carried out following the procedure described in UNE-EN ISO 2062: 2010. Uster Tensokid automatic dynamometer, model PE 4056 was used. The testXpert Standard v 6.01 software was used to obtain the stress-strain curves. System was set up to an elongation of 85% of the initial test piece.

RESULTS AND DISCUSSION

Effect of dispersing agents on CaF_2 NCPs

First, fluorite (CaF_2) nanoparticles (**Fig. 1**) were obtained by a wet chemical synthesis, as explained in a previous work[21]. Consecutively, PET/CaF_2 nanocomposite (NCP) samples were prepared with and without the different dispersing agents. With the aim to determine the effect of different dispersing agents on the crystallization behaviour of PET/CaF_2 NCPs, non-isothermal crystallization studies were carried out by Differential Scanning Calorimetry (DSC). Crystallization temperature (Tc) of the cooling process was calculated from the crystallization

peak of the resulting thermograms (**Fig. 2**). The addition of inorganic nanoparticles resulted in a relevant decrease of the Tc respect to the neat polymer due to an anti-nucleating effect of the CaF_2 in the matrix at the processing conditions, in opposite to the nucleating effect found on a previous study[21]. Nevertheless, preparation conditions of the composite were different, allowing a better mixing of the components. In this case, this fact could lead to a desaggregation of the loosely bound nanoparticles, producing new surfaces.

On the other hand, Tc values for PET/different dispersing agent samples appeared similar (PET/AW) or slightly above (PET/PSEMA and PET/MAWMA) respect to the one of pure PET. This fact may indicate that the presence of the agents in the polymer generate nucleation points, even though the increasing of Tc was around 2ºC. Besides, two different tendencies were spotted in NCP systems (**Fig. 2**). At first term, all Tc evolutions tended to shift down when cooling rate increased for all NCP systems. This observation may be explained by the formation of spherulites when rates are low as a result of longer exposure times to temperature, demonstrated in a previous work[21]. Moreover, NCP/PSEMA and NCP/AW Tc values evolved similarly to PET/CaF_2 sample. Nevertheless, the incorporation of MAWMA (NCP/MAWMA) improved significantly that value, however did not reach the neat polymer. Thus, the addition of MAWMA dispersing agent in PET/CaF_2 composites allowed the production of mixtures in conditions close to PET, which is very relevant from the industrial point of view. The better chemical compatibility between PET and particle due to the more lipohilic character of MAWMA was assumed, resulting in an enviornment of the composite close to the pure polymer.

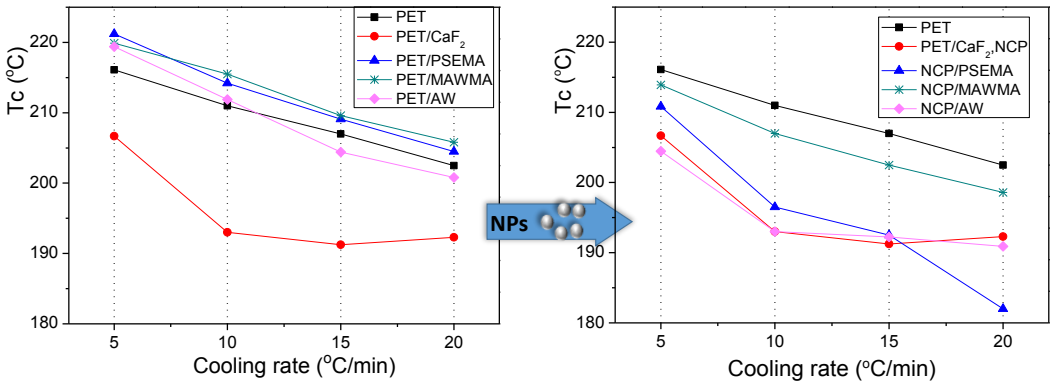

Fig. 2 *Evolutions of Tc at different cooling rates for (left) PET/dispersing agents and (right) NCP/dispersing agent.*

Furthermore, crystallization enthalpies (ΔHc) and standard deviation of them were calculated for all samples at all cooling rates (**Table 2**). ΔHc values were corrected according to exact weight of each sample. The incorporation of the dispersing agent to neat polyester did not produce important changes in the enthalpy of the samples when comparing with PET. A decrease, in absolute value of the ΔHc, corresponding to the area of the exothermic crystallization peak was revealed for all cooling times when CaF_2 nanoparticles were added to polymer. From all NCPs samples, NCP/MAWMA exhibited ΔHc values very close to PET, highlighting promising dispersing properties even at low cooling rates.

Table 2*. Mean values and standard deviation of ΔHc, for all the cooling rates, for all the samples.*

	ΔHc (J/g)

CaF_2 content	PET	PET + PSEMA	PET + MAWMA	PET + AW
0%	-57.0 ± 0.6	-59.6 ± 0.5	-58.3 ± 2.3	-57.1 ± 2.8
2%	-49.6 ± 3.2	-51.9 ± 2.0	-52,9 ± 2.0	-49.8 ± 2.0

The crystallization conversion degree (χ) was obtained by the calculation of the partial areas of the exothermic crystallization peak. The degree of crystallization at each cooling rate ($\chi(t)$) was determined by the integration of the partial crystallization exotherm, previously delimited. Delimitation was set by referencing the time at which crystallization begins (t_0) (**Eq.1**).

$$\chi(t) = \int_0^t (dH/dt) \cdot dt / \int_0^\infty (dH/dt) \cdot dt = \frac{\Delta H_t}{\Delta H_\infty} \qquad \textbf{\textit{Eq.1}}$$

where t corresponds to time and $\Delta H_t / \Delta H_\infty$ is the partial area of the exotherm of crystallization at a time t. Then, $\chi(t)$ in front of temperature and time for NCP samples were plotted (**Fig. 3**). The conversion was reported to be faster at higher cooling rates and, consequently, the phenomenon was initiated at lower temperatures than for the pure PET. This observation was in concordance with Tc evolution for all samples. The incorporation of CaF_2 and the dispersing agents to the neat polymer slightly delayed the starting point of the crystallization phenomenon in function of time, although the overall tendency was found very similar. This behaviour appeared almost identical for the rest of the samples.

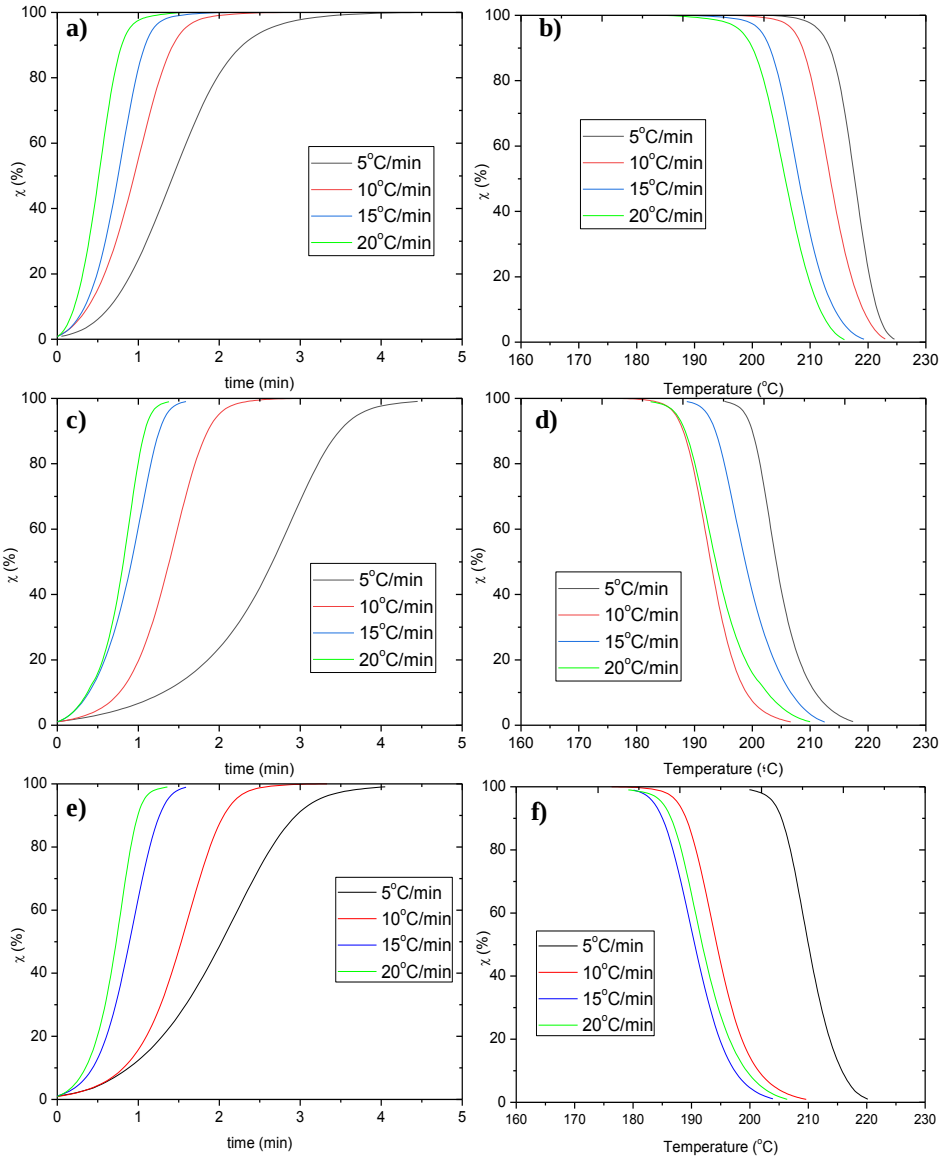

Fig. 3 *Evolutions of the relative crystallinity (χ) with time (a, c and e) and temperature (b, d and f) of PET (a and b), PET/CaF_2 (c and d) and NCP/MAWMA (e and f) at different constant cooling rates.*

In order to calculate kinetic parameters for describing non-isothermal crystallization, Avrami's model[23], was applied (**Eq. 2**).

$$\chi = 1 - \exp(Z_t \cdot t^n) \qquad \textbf{\textit{Eq.2}}$$

where n exponent is a constant mechanism (with variations from 1 to 4). n value is depending on the type of nucleation (homogeneous or heterogeneous) and on the growing process parameters (1D, 2D or 3D)[24]. On the other hand, Z_t corresponds to a constant rate that includes both, the nucleation parameter and the growth rate. By developing **Eq.2**, appears **Eq. 3**.

$$\ln[-\ln(1-\chi)] = n \cdot \ln t + \ln Z_t \qquad \textbf{\textit{Eq.3}}$$

With the objective to determine the kinetic parameters n and Z_t form **Eq. 3**, $\ln[-\ln(1-\chi)]$ *vs.* $\ln t$ was plotted (**Fig. 4**). Avrami's relation showed that MAWMA NCP evolved similarly to neat

PET for all cooling rates, excepting for 15 and 20ºC/min which was in concordance with previous results. This fact corroborated that esters of montanic acid enhance nucleation properties of CaF_2 when added to PET at high cooling rates.

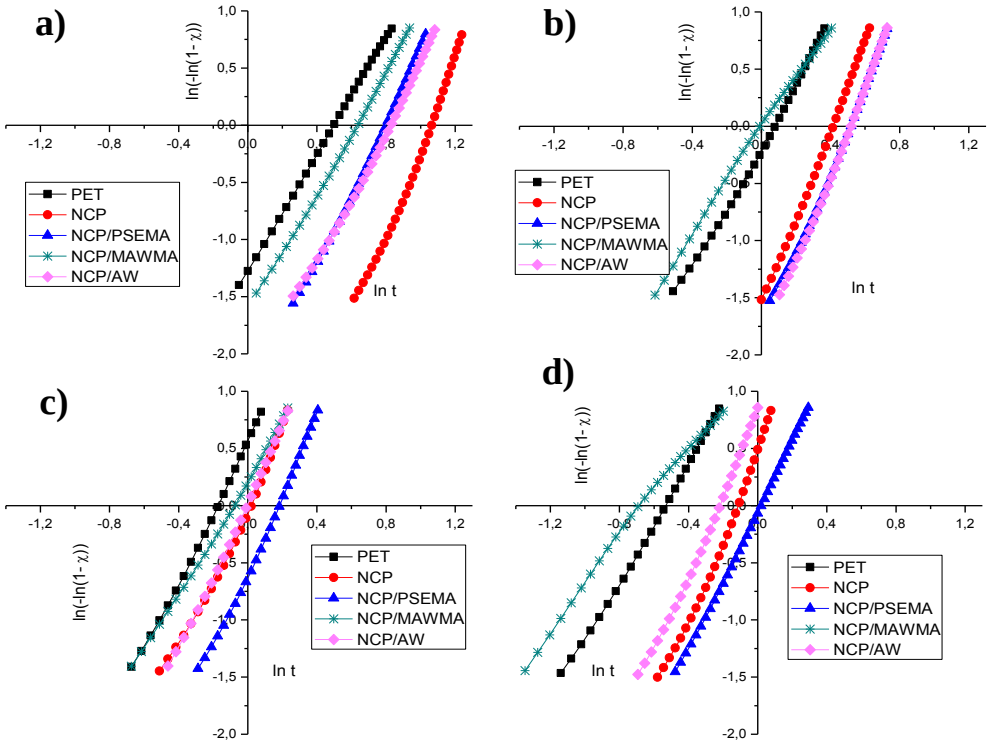

Fig. 4 *Avrami's relation of PET and NCPs at a)5ºC/min, b) 10ºC/min, c) 15ºC/min and d) 20ºC/min.*

Avrami kinetic parameter, n, showed regular values within a same system regardless of the cooling rate and of the dispersing agent (**Table 3**). n values were found between 2 and 3.5, indicating an heterogeneous nucleation, and the formation of 3D spherulites[24]. Actually, n values exhibited two tendencies, one followed by PET and NCP/MAWMA and, another followed by the rest of the three mixtures. Consequently, MAWMA dispersing agent allowed to produce composite systems with similar nucleation behaviour as PET, confirming promising properties of NCP/MAWMA samples at industrial level.

Table 3*. Avrami kinetic parameter n of PET, PET/CaF_2 and NCP/dispersing agents at different cooling rates.*

α (ºC/min)	**PET**	**PET/CaF_2**	**NCP/*PSEMA***	**NCP/*MAWMA***	**NCP/*AW***
5	2.60	3.25	3.13	2.64	2.97
10	2.91	3.20	3.51	2.30	3.55
15	3.00	3.24	3.36	2.42	3.37
20	2.59	3.45	3.24	1.92	2.99

On the other hand, Z_t (**Table 4**) increased with the cooling rate probably due to crystallization occurred faster at lower temperatures.

Table 4*. Avrami kinetic parameters Z_t (min^{-n}) of PET, PET/CaF_2 and NCP/dispersing agents at different cooling rates.*

α (ºC/min)	PET	PET/CaF_2	NCP/*PSEMA*	NCP/*MAWMA*	NCP/*AW*
5	0.27	0.07	0.08	0.19	0.07
10	0.65	0.87	0.19	0.95	0.18
15	1.71	0.99	0.70	1.24	0.86
20	3.83	1.62	1.46	2.96	1.64

Nevertheless, Jeziorny characterized non-isothermal crystallization by correcting the Avrami's model parameters (**Eq. 4**)[25].

$$\ln Z_c = \frac{\ln Z_t}{\alpha} \qquad \textit{Eq.4}$$

where α corresponds to the cooling rate and Z_c is the corrected crystallization constant (**Table 5**). Theoretically, Z_c should be independent of cooling rate, however this affirmation was not true for all rates. Z_c mean values for all the composites were 0.65 ± 0.09 min^{-n} at a cooling rate of 5ºC/min and 0.99 ± 0.07 min^{-n} for 10, 15 and 20ºC/min.

***Table 5**. Avrami kinetic parameters Zc of PET, PET/CaF_2 and NCP/dispersing agents at different cooling rates.*

α (ºC/min)	PET	PET/CaF_2	NCP/*PSEMA*	NCP/*MAWMA*	NCP/*AW*
5	0.77	0.60	0.60	0.72	0.58
10	0.96	0.99	0.85	1.00	0.84
15	1.04	1.00	0.98	1.01	0.99
20	1.07	1.02	1.02	1.06	1.03

In this way, the calculation of the half crystallization time ($t^{1/2}$) could be accomplished by determining the time needed to reach 50% of crystallization. Furthermore, $t^{1/2}$ appeared in concordance with the behaviour reported above (**Fig. 5**). $t^{1/2}$ evolved similarly for PET and NCP/MAWMA samples, however underneath of the rest of the composites, and it seemed that tended to keep a constant tendency at higher cooling rates. Thus, the presence of the ester wax in PET/CaF_2 blends enabled a more homogeneous dispersion and more intimate mixture, resulting in a nucleating behaviour of the fluorite nanoparticles to the system, more similar to the one observed in previous studies[11]. On the other hand, the presence of AW and PSEMA into de NCP raised $t^{1/2}$ above from the original PET up to similar levels of plain NCP. In this way, a slower crystallization reaction when CaF_2 is added to PET, even after the addition of AW and PSEMA, could be concluded. However, the anti-nucleating behaviour of CaF_2 seemed to be smoothed in presence of the more lipophilic MAWMA (NCP/MAWMA), having a crystallization rate almost the same as PET.

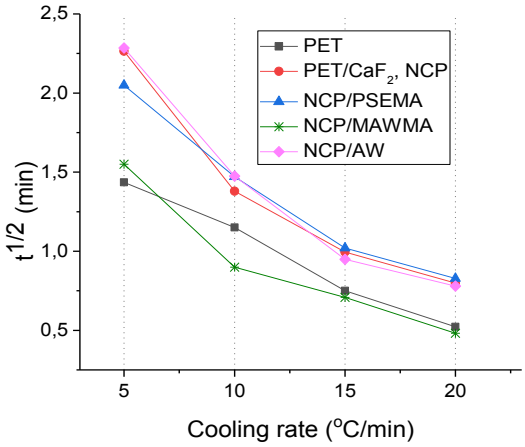

Fig. 5 *Evolution of half crystallization time with cooling rate of substrates with and without CaF_2 and in the presence of the dispersing agents.*

Furthermore, Birefringence Optical Microscopy (BOM) was carried out for the evaluation of the dispersing effect of the different additives (**Fig. 6**). The dispersing effect on CaF_2 of the composite after the addition of the dispersing agents was clearly spotted, where differences on the level of nanoparticle aggregation were evident by the appearance of bright spots in some of the samples. NCP/AW and NCP/MAWMA showed a more homogeneous distribution of the particles. As established by Paul and Newman[26], compatibility of the components in the polymeric mixture is defined mostly by the chemical structure. If the particle coating (surfactant) has an adequate chemical affinity for the polymer, aggregation of the filling can be avoided.

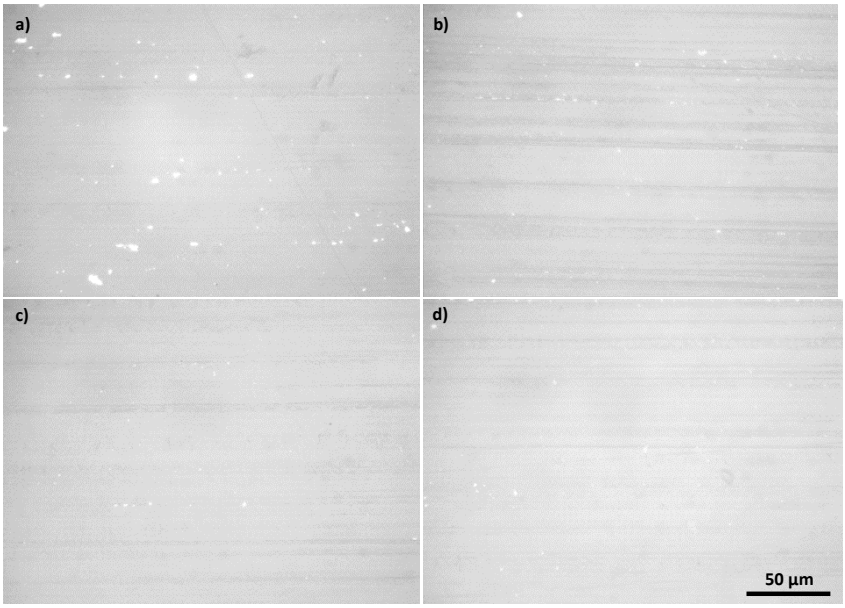

Fig. 6 *BOM images from a) NCP, b) NCP/PSEMA, c) NCP/AW and d) NCP/MAWMA.*

Effect of CaF_2 particle size on NCP

Afterwards, the study about the influence of the particle size and concentration on the NCP was carried out. To do this, MAWMA was the selected dispersing agent because it revealed as the

most promising dispersant, according to the previous results. On the other hand, textile PET previously used was replaced by a more suitable PET for moulding.

DSC technique was used for the study of the thermal behaviour of the micro- and nano-composites microstructure. First, samples were heated up to 290ºC to 'clean' the thermal history of the samples, then cooled at 20ºC/min to record differences in the non-isothermal crystallization behaviour and heated again to determine the melting behaviour of each sample. In this case, the same 'thermal memory' will be imprinted in the cooling to all composites and thermal variations will be only related to changes in composition and particle size (**Fig. 7**).

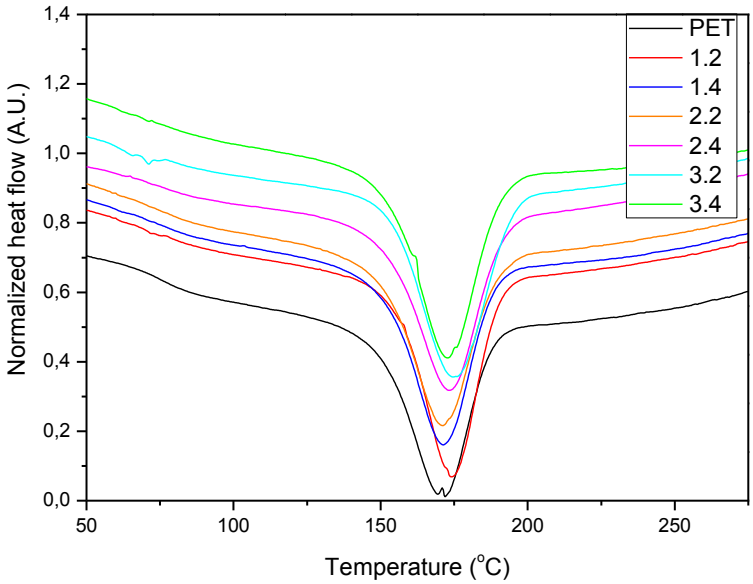

Fig. 7 *Cold crystallization areas from DSC thermograms of PET and NCP samples. NOTE: first number corresponds to CaF_2 (%) content and the second to MAWMA (%) content.*

After obtaining all thermograms, Tc and ΔHc values were calculated (**Table 6**). Tc increased after the addition of CaF_2 for all samples, excepting for microparticles containing the highest concentration of MAWMA. According to Serenko *et al.*, this observation would be related with the presence of an organic layer of dispersing agent on the surface of CaF_2, which increases the degrees of freedom and, consequently, the system entropy[27]. Nanoparticulated CaF_2 increased Tc respect to micro-CaF_2, however the tendency was inverted when 3% CaF_2 was reached, corroborating the high dispersion capacity of MAWMA in the NCP system. On the other hand, no clear tendency could be extracted with ΔHc values.

Table 6. *Tc and ΔHc values calculated from the non-isothermal crystallization thermograms for all the samples.*

CaF_2 (%)		**MAWMA concentration: 2%**		**MAWMA concentration: 4%**	
		Tc (ºC)	**ΔHc (J/g)**	**Tc (ºC)**	**ΔHc (J/g)**
Microparticles	**1**	172.2	-45.8	169.6	-44.5
	2	170.6	-44.7	169.1	-46.8
	3	179.5	-48.6	178.7	-50.0
Nanoparticles	**1**	174.3	-45.5	171.6	-44.7
	2	171.4	-44.9	173.3	-46.2
	3	174.6	-48.1	172.6	-47.8
PET		171.6	-47.5		

The dependence of the glass transition temperatures (Tg) and heat capacities (ΔCp) of the micro- and nano-composites on the filler concentration and their size are shown in **Table 7**. Thermal analyses indicated that Tg values decreased with the increase of CaF_2 particle concentration and with the amount of dispersing agent, and was especially relevant for samples with 3% of CaF_2. Zhiltsow *et al.* claimed that the Tg significantly decreases with the decrease of the level of thermodynamic compatibility between the polymer and the particles surface coating[29]. Thus, an adequate compatibility would be translated in a moderate decrease of the Tg when particles are introduced to the matrix, however in less proportion than in the case where particles possess limited compatibility. Simulation studies concluded that Tg decreases and polymer chain mobility close to the interface increases if the attractive polymer/substrate interaction becomes weaker[30,31]. In this work, Tg values were not significantly influenced by the particle size or the dispersant concentration, but was greatly influenced by the filler concentration. Thus, an increase of the spacing between macromolecular chains as a result of the occupation of amorphous spaces in the amorphous regions of polymer by nanoparticles and, a subsequent decrease of the overall Tg, could be concluded[27]. The presence of the dispersing agent accentuated that behaviour, providing plasticity to the polymer and decreasing the entropy of the system, compared with PET/CaF_2[27]. Furthermore, no significant correlations between ΔCp with size and concentration of CaF_2 and MAWMA could be established.

***Table 7**. Microstructure behaviour, in the glass transition region, of PET, PET/CaF_2 and NCP/dispersing agent obtained from DSC technique.*

CaF_2 (%)		**MAWMA concentration: 2%**		**MAWMA concentration: 4%**	
		Tg (ºC)	**ΔCp (J/g·ºC)**	**Tg (ºC)**	**ΔCp (J/g·ºC)**
Microparticles	**1**	76.8	0.14	76.5	0.13
	2	75.9	0.11	75.3	0.12
	3	69.9	0.13	69.5	0.06
Nanoparticles	**1**	76.8	0.13	77.5	0.16
	2	76.0	0.17	76.6	0.17
	3	72.1	0.12	69.8	0.13
PET		79.6	0.12		

On the other hand, melting temperatures (Tm) did not change significantly with size and concentration of CaF_2 and MAWMA, probably due to the amount of additive which was insufficient to change this parameter (**Table 8**). Enthalpy values of the melting peaks were corrected by taking into account the true percentage of polyester in the mixture (ΔHm). ΔHm increased for all NCPs respect to PET and, although a clear tendency between CaF_2 size and content could not be established, enthalpy and, therefore, crystallinity increased a 37% in the sample with the highest content of MAWMA and CaF_2.

***Table 8**. Microstructure behaviour, in the melting region, of PET, PET/CaF_2 and NCP/dispersing agent obtained from DSC technique.*

CaF_2 (%)		**MAWMA concentration: 2%**		**MAWMA concentration: 4%**	
		Tm (ºC)	**ΔHm (J/g)**	**Tm (ºC)**	**ΔHm (J/g)**
Microparticles	**1**	246.3	38.64	246.3	43.26
	2	247.3	46.13	246.3	47.40
	3	245.3	49.26	246.0	45.37
Nanoparticles	**1**	246.7	43.47	245.3	42.84
	2	246.3	52.47	245.3	42.06

	3	246.7	44.42	245.0	55.36
PET		246.0	40.42		

CaF_2 NCP multifilament

Once micro- and nano-composites were analysed in plate form, studies were focused towards the obtaining of hybrid fibres with textile characteristics. From the previous results, no significant differences were observed when studying different concentrations of CaF_2 and dispersing agent for industrial applications. However, some discontinuities at the exit of the extruder when the content of particles was 3% were reported. For those reasons and due to economic criteria, the fabrication of NCP yarns containing 2% CaF_2 and 2% MAWMA was proposed for the analysis in this section. In the preparation of the yarn, the use of micrometric fluorite was not possible for spinning because of the very low viscosity of the spinning fluid. Thus, only CaF_2 nano-particles were used to produce hybrid multifilament. With the aim to develop this, PET polymer was extruded with and without the inclusion of nano-particles to obtain POY (Partially Oriented Yarn) multifilament and then, the yarn stretched with a drawn ratio of 1:2.

Molecular weight determinations of PET and NCP multifilament yarns revealed that the inclusion of ceramic particles decreases both, average molecular weight in number (Mn) and average molecular weight in weight (Mw) (**Table 9**) as consequence of the reduction of the intrinsic viscosity of the polymer (matrix) because of higher temperature and higher shear rate exposures and, long residence times during the extrusion process[6].

Table 9*. GPC and mechanical assay results of PET and NCP/MAWMA yarns (CV of the mechanical tests are in parenthesis).*

	GPC			**Mechanical parameters**	
Yarn	**Mn (kg/mol)**	**Mw (kg/mol)**	**Mw/Mn**	**Tenacity (cN/tex)**	**Maximum elongation (%)**
PET	27.6	51.5	2.0	35.9 (4.4%)	23.1 (9.6%)
NCP/MAWMA	20.4	39.9	2.1	28.5 (7.5%)	21.9 (13.8%)

Generally, polyester fibres have relevant and valuable mechanical properties that are closely related with the nucleation process, whereby primary nuclei of crystals are formed. If molecular movements of polymer in melted state allow alignment of enough chain segments, then nuclei formation phenomenon develops homogeneously. Otherwise, during that process nuclei are formed by the contact between substance and, either the walls of the container where the substance is in in, or the insoluble microscopic particles randomly distributed into the material.[32] Mechanical assays showed that the effect of inclusion of ceramic particles to PET decreased the tenacity of composed fibres compared to pure polymer, and that this phenomenon could be related to the decrease of the molecular weight of the composites (**Table 9**). The presence of nanoparticles would difficult the movement of the macromolecular chains of PET, resulting in a decrease of the tenacity and maximum elongation value as confirmed by mechanical assays (**Table 9**). In addition, CaF_2 particles may also act as stress concentration sites in the composites. Bigger particles induce higher stress concentrations into the matrix and also lead to a reduction

in impact energy. As a result, crack propagation could initiate locally, and, the final failure appears earlier[33–35].

CONCLUSIONS

A novel hybrid filament of NCP/MAWMA has been developed. In first term, non-isothermal crystallization behaviour of NCP with different dispersing agents in plate form has been studied by DSC at different cooling rates in order to determine the most suitable system. Thermograms have revealed a decrease of Tc when CaF_2 was added to polymer for all samples, due to the anti-nucleating behaviour of the ceramic nanoparticles in the conditions of the study. Extensively, a subtle dispersing effect of PSEMA and AW has been observed due to similarities in the Tc evolution between PET/CaF_2 and, NCP/PSEMA and NCP/AW samples. Nevertheless, NCP/MAWMA has shown very similar behaviour to plain PET, which is relevant for industrial applications. ΔHc of NCP/MAWMA has appeared to evolve closely to PET even at low cooling rates, in concordance with the results. That means that the anti-nucleating effect of CaF_2, that may difficult the production of the hybrid multifilament, has been neutralized by the addition of MAWMA. MAWMA acts as a coating highly compatible with the polymer.

Avrami kinetic parameter, n, has resulted in almost regular values for a given sample, independently of the cooling rate and dispersing agent. Those values have found to be 2-3.5 indicating an heterogeneous nucleation and the formation of 3D spherulites during the crystallization process. Moreover, n has revealed that PET and NCP/MAWMA have behaved very similar during nucleation process. Additionally, the values of $t^{1/2}$ has been increased by the presence of PSEMA and AW to NCP samples, contrarily to MAWMA, corroborating that NCP/MAWMA is a promising system.

On the other hand, BOM images have allowed to appreciate some differences in the dispersion degree between the different NCP samples. Due to favourable results with NCP/MAWMA, the influence of particle size and the concentration of CaF_2 and dispersing agent has been evaluated by DSC. Samples with micro-CaF_2 have denoted a general decrease of the Tg whereas by nano-sized particles this was increased, confirming a better dispersion degree for NCP due to a lower entropy of the system. Furthermore, an inverse relation between the Tg and concentrations of CaF_2 and MAWMA, specially at 3% of dispersing agent, was found. However, no significant correlation between thermal parameters of CaF_2 size and concentration and MAWMA could be established.

Finally, PET POY multifilament containing 2% of nano-CaF_2 and 2% MAWMA has been obtained. GPC technique has shown very similar polydispersity values for NCP/MAWMA yarn respect to pure PET yarn, confirming previously observations made by plate samples. Regarding mechanical assays, a tenacity value of 28.5 cN/tex and a maximum elongation of 21.9% have been found for NCP/MAWMA multifilament system.

NCP/MAWMA multifilament constitutes a new composite system with high degree of nano-particle dispersion. Results demonstrate that the nano-composite can be thermally processed as PET, which is promising and valuable from the industrial point of view.

ACKNOWLEDGEMENTS

Authors gratefully acknowledge the financial support for this research from the Ministry of Science and Innovation of Spain (Project MAT2010-20324-CO2-01) and from the National Secretary of Higher Education Science Technology and Innovation of Ecuador (SENESCYT) for Master's Fellowship (No. 2015-AR2Q8981). Also, authors would like to thank to the companies ANTEX, S.L. and La Seda de Barcelona for providing the different polyester pellets and, Clariant for providing the dispersing agents and to IQAP Masterbatch Group S.L. for the production of the hybrid multifilaments. Finally, authors acknowledge Mrs. Carmen Escamilla and Mrs. Montserrat García for their support in the experimental work.

DATA AVAILABILITY

The raw/processed data required to reproduce these findings cannot be shared at this time as the data also forms part of an ongoing study.

REFERENCES

1. Kumar, S. K. & Krishnamoorti, R. Nanocomposites: Structure, Phase Behavior, and Properties. *Annu. Rev. Chem. Biomol. Eng.* **1**, 37–58 (2010).
2. Carosio, F., Alongi, J. & Frache, A. Influence of surface activation by plasma and nanoparticle adsorption on the morphology, thermal stability and combustion behavior of PET fabrics. *Eur. Polym. J.* **47**, 893–902 (2011).
3. Ji, Q., Wang, X., Zhang, Y., Kong, Q. & Xia, Y. Characterization of Poly (ethylene terephthalate)/SiO2 nanocomposites prepared by Sol–Gel method. *Compos. Part A Appl. Sci. Manuf.* **40**, 878–882 (2009).
4. Joshi, M. & Bhattacharyya, A. Nanotechnology – a new route to high-performance functional textiles. *Text. Prog.* **43**, 155–233 (2011).
5. Wang, P., Dong, Y., Li, B., Li, Z. & Bian, L. A sustainable and cost effective surface functionalization of cotton fabric using TiO2 hydrosol produced in a pilot scale: Condition optimization, sunlight-driven photocatalytic activity and practical applications. *Ind. Crops Prod.* **123**, 197–207 (2018).
6. Todorov, L. V., Martins, C. I. & Viana, J. C. Characterization of PET Nanocomposites with Different Nanofillers. *Solid State Phenom.* **151**, 113–117 (2009).
7. Estrada, M. R., Calderas, F. & Manero, O. Mechanical and Rheological Studies on Polyethylene Terephthalate - Montmorillonite Nanocomposites. *Sci. Technol.* **2003**, (2003).
8. Sabetghadam, A. *et al.* Metal Organic Framework Crystals in Mixed-Matrix Membranes: Impact of the Filler Morphology on the Gas Separation Performance. *Adv. Funct. Mater.* **26**, 3154–3163 (2016).
9. Sun, K. *et al.* Flexible polydimethylsiloxane/multi-walled carbon nanotubes membranous metacomposites with negative permittivity. *Polymer (Guildf).* **125**, 50–57 (2017).
10. Zhao, S. *et al.* The Crystallization Behavior of Isotactic Polypropylene Induced by a Novel Antinucleating Agent and Its Inhibition Mechanism of Nucleation. *Ind. Eng. Chem. Res.* **54**, 7650–7657 (2015).
11. Cayuela, D., Cot, M., Algaba, I. & Manich, A. M. Effect of different dispersing agents in the non-isothermal kinetics and thermomechanical behavior of PET/TiO 2 composites. *J. Macromol. Sci. Part A* **53**, 237–244 (2016).
12. Zhang, G., Xu, C., Wu, D., Xie, W. & Wang, Z. Crystallization of Green Poly(ε-caprolactone) Nanocomposites with Starch Nanocrystal: The Nucleation Role Switching of Starch Nanocrystal with Its Surface Acetylation. *Ind. Eng. Chem. Res.* **57**, 6257–6264 (2018).
13. Zhang, X. *et al.* Highly Uniform and Monodisperse Ba(2)CIF(3) Microrods: Solvothermal Synthesis and Characterization. *Cryst. Growth Des.* **8**, (2008).
14. Gao, P., Xie, Y. & Li, Z. Controlling the Size of BaF2 Nanocubes from 1000 to 10 nm. *Eur. J. Inorg. Chem.* **2006**, 3261–3265 (2006).
15. Pandurangappa, C., Lakshminarasappa, B. N. & Nagabhushana, B. M. Synthesis and characterization of CaF2 nanocrystals. *J. Alloys Compd.* **489**, 592–595 (2010).
16. Petit, V., Doualan, J. L., Camy, P., Ménard, V. & Moncorgé, R. CW and tunable laser operation of Yb3+ doped CaF2. *Appl. Phys. B* **78**, 681–684 (2004).
17. Lucca, A. *et al.* High-power tunable diode-pumped Yb^3+:CaF_2 laser. *Opt. Lett.* **29**, 1879 (2004).
18. Wang, L., Wang, B., Wang, X. & Liu, W. Tribological investigation of CaF2 nanocrystals as grease additives. *Tribol. Int.* **40**, 1179–1185 (2007).
19. Sánchez-Leija, R. J., Riba-Moliner, M., Cayuela-Marín, D., Domínguez-Espinós, O. & Sánchez-Loredo, M. G. Surface modification of a calcium fluoride filler and the effect on the nonisothermal crystallization behavior of poly(ethylene terephthalate). *Polym. Eng. Sci.* **54**, 2938–2946 (2014).
20. Surface Modification of a Calcium Fluoride Filler and theEffect on the Nonisothermal Crystallization Behavior ofPoly(ethylene terephthalate).pdf.

21. Sánchez-Leija, R. J., Riba-Moliner, M., Cayuela-Marín, D., Domínguez-Espinós, O. & Sánchez-Loredo, M. G. Surface effect of two different calcium fluoride fillers on the non-isothermal crystallization behavior of poly(ethylene terephthalate). *J. Macromol. Sci. Part B* **53**, 173–190 (2014).
22. Gacén Esbec, I. Modificación de la estructura fina de la fibras de PET en el termofijado y en su tintura posterior. Tintura competitiva de sustratos termofijados a temperaturas vecinas. (Universidad Politécnica de Cataluña, 2004).
23. Avrami, M. Kinetics of Phase Change. I General Theory. *J. Chem. Phys.* **7**, 1103–1112 (1939).
24. Avrami, M. Kinetics of Phase Change. II Transformation-Time Relations for Random Distribution of Nuclei. *J. Chem. Phys.* **8**, 212–224 (1940).
25. Jeziorny, A. Parameters characterizing the kinetics of the non-isothermal crystallization of poly(ethylene terephthalate) determined by DSC. *Polymer (Guildf).* **19**, 1142–1144 (1978).
26. Paul, D. R. & Newman, S. *Polymer Blends*. (Elsevier Science, 1978).
27. Serenko, O. A. *et al.* The effect of size and concentration of nanoparticles on the glass transition temperature of polymer nanocomposites. *RSC Adv.* **7**, 50113–50120 (2017).
28. Vassiliou, A. A., Chrissafis, K. & Bikiaris, D. N. In situ prepared PET nanocomposites: Effect of organically modified montmorillonite and fumed silica nanoparticles on PET physical properties and thermal degradation kinetics. *Thermochim. Acta* **500**, 21–29 (2010).
29. Zhiltsov, A. *et al.* Polylactide and hybrid silicasol nanoparticle-based composites. *J. Appl. Polym. Sci.* **132**, (2015).
30. Tanaka, K. *et al.* Interfacial Mobility of Polymers on Inorganic Solids. *J. Phys. Chem. B* **113**, 4571–4577 (2009).
31. Morita, H., Tanaka, K., Kajiyama, T., Nishi, T. & Doi, M. Study of the Glass Transition Temperature of Polymer Surface by Coarse-Grained Molecular Dynamics Simulation. *Macromolecules* **39**, 6233–6237 (2006).
32. Peacock, A. J. & Calhoun, A. R. *Polymer Chemistry: Properties and Applications*. (Hanser Gardner Publications, 2006).
33. Shayestehfar, S., Yazdanshenas, M. E., Khajavi, R. & Rashidi, A. S. Physical and Mechanical Properties of Nylon 6/ Titanium Dioxide Micro and Nano-Composite Multifilament Yarns. *J. Eng. Fiber. Fabr.* **9**, 158–167 (2014).
34. Selvin, T. P., Kuruvilla, J. & Sabu, T. Mechanical properties of titanium dioxide-filled polystyrene microcomposites. *Mater. Lett.* **58**, 281–289 (2004).
35. Burke, M., Young, R. J. & Stanford, J. L. The relationship between structure and properties in titanium dioxide filled polypropylene. *Polym. Bull.* **30**, 361–368 (1993).